Defective transcription initiation causes postnatal growth failure in a mouse model of nucleotide excision repair (NER) progeria

Irene Kamileri[a,b], Ismene Karakasilioti[a,b], Aria Sideri[a], Theodoros Kosteas[a], Antonis Tatarakis[c], Iannis Talianidis[c], and George A. Garinis[a,b,1]

[a]Institute of Molecular Biology and Biotechnology, Foundation for Research and Technology-Hellas, Nikolaou Plastira 100, 70013, Heraklion, Crete, Greece; [b]Department of Biology, University of Crete, Vassilika Vouton, GR71409, Heraklion, Crete, Greece; and [c]Biomedical Sciences Research Center Al. Fleming, 16672 Vari, Greece

Edited by Philip C. Hanawalt, Stanford University, Stanford, CA, and approved January 17, 2012 (received for review September 10, 2011)

Nucleotide excision repair (NER) defects are associated with cancer, developmental disorders and neurodegeneration. However, with the exception of cancer, the links between defects in NER and developmental abnormalities are not well understood. Here, we show that the ERCC1-XPF NER endonuclease assembles on active promoters in vivo and facilitates chromatin modifications for transcription during mammalian development. We find that *Ercc1*$^{-/-}$ mice demonstrate striking physiological, metabolic and gene expression parallels with *Taf10*$^{-/-}$ animals carrying a liver-specific transcription factor II D (TFIID) defect in transcription initiation. Promoter occupancy studies combined with expression profiling in the liver and in vitro differentiation cell assays reveal that ERCC1-XPF interacts with TFIID and assembles with POL II and the basal transcription machinery on promoters in vivo. Whereas ERCC1-XPF is required for the initial activation of genes associated with growth, it is dispensable for ongoing transcription. Recruitment of ERCC1-XPF on promoters is accompanied by promoter-proximal DNA demethylation and histone marks associated with active hepatic transcription. Collectively, the data unveil a role of ERCC1/XPF endonuclease in transcription initiation establishing its causal contribution to NER developmental disorders.

DNA damage | genetics | metabolism

Developmental-stage and tissue-specific programs of gene expression require the action of sequence-specific DNA binding factors, the basal transcription machinery and chromatin remodeling and modification enzymes (1). Together, these factors create a chromatin environment that allows the synthesis of the primary transcript (2). If the transcriptional machinery is defective or challenged due to e.g., transcription-blocking DNA lesions, the process of RNA synthesis halts. To ensure that the genetic information is preserved and that transcription is not compromised, cells use DNA repair systems aimed at counteracting DNA damage (3). For bulky helix-distorting damage, the principal repair mechanism is the evolutionarily conserved nucleotide excision repair (NER) pathway. NER operates via a "cut and patch" type of mechanism involving ~30 proteins that recognize and remove helical distortions throughout the genome (global genome NER; GGR), or selectively from the transcribed strand of active genes (transcription-coupled repair; TCR) (4). In GGR, the DNA is surveyed by the XPC-hR23B complex and the UV-damaged DNA-binding protein. Instead, damage recognition in TCR requires the RNA polymerase II (POL II), CSA, and CSB. Unwinding the DNA around a lesion and stabilization of single-stranded DNA is followed by the XPG and ERCC1-XPF endonucleases that cleave on the 3′ and 5′side of the DNA lesion, respectively followed by excision of the damage and gap-filling DNA synthesis (5).

Inborn NER defects may lead to skin cancer-prone xeroderma pigmentosum (XP) (6) or to a heterogeneous group of developmental disorders, including Cockayne syndrome (CS; affected genes: *Csb* and *Csa*) and trichothiodystrophy (TTD; affected genes: *Xpd* and *Xpb*) (7). CS and TTD patients are characterized by postnatal growth failure, skeletal and neuronal abnormalities, s.c. fat loss and short lifespan (collectively designated as "segmental" NER progeroid features), but not cancer (8). Mouse mutants with inborn NER defects closely mimic their human counterparts and display severe developmental abnormalities and short lifespan (9).

Whereas defective NER of damaged DNA has been established as the underlying cause of mutations leading to skin cancer, the links between NER defects and the developmental abnormalities seen in NER disorders remain unclear (10–12). Earlier studies have shown that distinct NER factors play a role in transcription (5, 13, 14) and that, upon stimulation, they are recruited to active promoters in vitro (15). However, the in vivo relevance of NER-mediated transcription to the NER developmental disorders remains elusive, primarily due to difficulties in dissecting the dual role of NER in DNA repair and transcription in an intact organism. Here, we provide evidence that key developmental abnormalities associated with a defect in NER originate from defective transcription initiation of gene expression programs.

Results

***Ercc1*$^{-/-}$ Mice Demonstrate Physiologic and Metabolic Parallels with Liver-Specific *Taf10*$^{-/-}$ Mice.** To assess the contribution of NER in transcription during development, we compared the liver phenotypes of NER-deficient *Ercc1*$^{-/-}$ animals that closely mimic a severe form of CS (11) with transcription factor II D (TFIID)-defective *Taf10*$^{-/-}$ mice exhibiting a liver-specific defect in transcription initiation (*Taf10*$^{-/-}$*-Alb-Cre*) (16). *Ercc1*$^{-/-}$ mice show attenuated growth, resulting in cachectic dwarfism during the second week of life and premature death before postnatal day P35 (Fig. 1*A*) (11). Likewise, liver-specific disruption of *Taf10* gene in *Taf10*$^{-/-}$ animals leads to severe growth failure during the second week after birth, more than 50% reduction in body weight at day P30, and premature death at ~P35 (Fig. 1*C*) (16). Oil Red O and PAS staining in *Ercc1*$^{-/-}$ and *Taf10*$^{-/-}$ livers revealed a uniform accumulation of triglycerides and glycogen resulting in a "fatty liver" appearance with unusually large glycogen depots (Fig. 1 *B* and *D*). Apoptosis was considerably higher in both animal models compared with controls (Fig. 1 *A*–*D Lower*). Thus, NER-defective *Ercc1*$^{-/-}$ mice and *Taf10*$^{-/-}$ animals deficient in transcription initiation share striking growth and metabolic abnormalities during postnatal development.

Author contributions: G.A.G. designed research; I. Kamileri, I. Karakasilioti, A.S., T.K., and G.A.G. performed research; A.T. and I.T. contributed new reagents/analytic tools; I.T. and G.A.G. analyzed data; and G.A.G. wrote the paper.

The authors declare no conflict of interest.

This article is a PNAS Direct Submission.

Data deposition: Microarray data have been deposited and are available at ArrayExpress (accession nos. E-MEXP-1503, E-MEXP-835, and E-MEXP-3442).

[1]To whom correspondence should be addressed. E-mail: garinis@imbb.forth.gr.

This article contains supporting information online at www.pnas.org/lookup/suppl/doi:10.1073/pnas.1114941109/-/DCSupplemental.

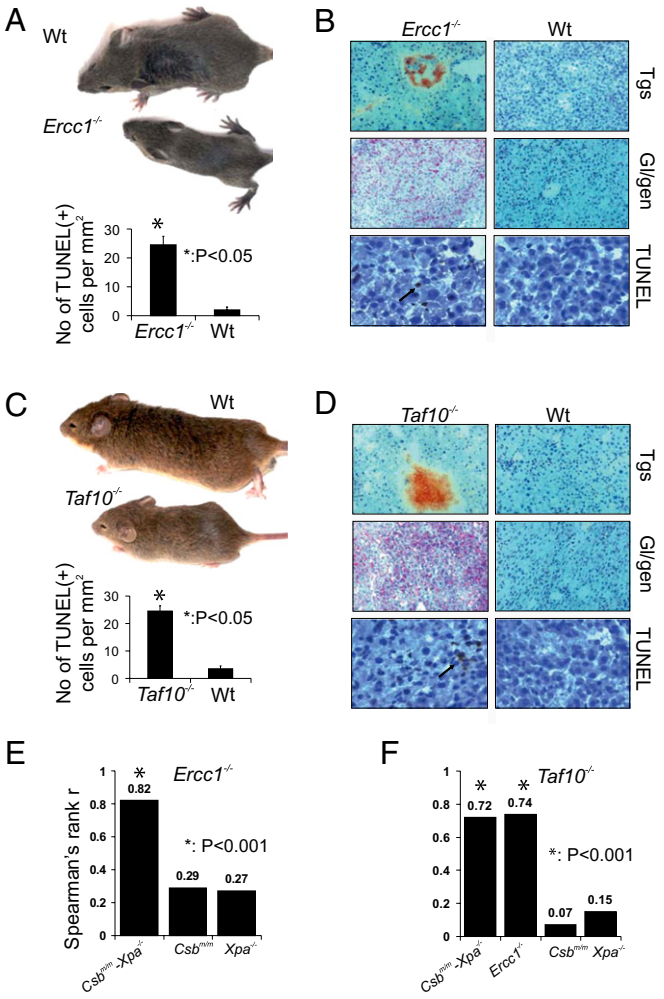

Fig. 1. Physiologic and transcriptome similarities between *Ercc1*$^{-/-}$ and *Taf10*$^{-/-}$ animals. (*A*) Photograph of P20 *Ercc1*$^{-/-}$ and wt animals. (*B*) Detection of triglycerides (TGs), glycogen (Gl/gen) at 20× magnification, and apoptosis at 40× magnification in P20 wt and *Ercc1*$^{-/-}$ livers, respectively. Quantification of TUNEL-positive cells (arrow) is shown in *A Lower*. (*C*) Photograph of P30 liver-specific *Taf10*$^{-/-}$ and wt animals. (*D*) Same as in *B*. (*E*) Spearman's *r* transcriptome similarities between the P15 *Ercc1*$^{-/-}$, or (*F*) the P30 *Taf10*$^{-/-}$ and the animal models shown in *x* axis; −1.0 is an inverse correlation, 0.0 is no correlation, and 1.0 is a perfect positive correlation. Error bars indicate SEM. Asterisks indicate statistically significant differences (two-tailed $P \leq 0.05$).

Genome-Wide Hepatic Gene Expression Similarities Between *Ercc1*$^{-/-}$ and *Taf10*$^{-/-}$ Animals. Using independent liver gene expression datasets and genomics approaches (*SI Appendix*) (17), we next evaluated the gene expression similarities between the livers of age-matched NER mutants (*SI Appendix*) displaying severe (*Csb*$^{m/m}$/*Xpa*$^{-/-}$, *Ercc1*$^{-/-}$), mild (*Csb*$^{m/m}$), or no significant (*Xpa*$^{-/-}$) growth defects. The *Ercc1*$^{-/-}$ transcriptome closely resembled that of the *Csb*$^{m/m}$/*Xpa*$^{-/-}$ cachectic dwarfs but not that of the growth-proficient *Csb*$^{m/m}$ or *Xpa*$^{-/-}$ mice (Fig. 1*E*). Similarly, the *Taf10*$^{-/-}$ liver transcriptome was strikingly similar to that of *Ercc1*$^{-/-}$ or *Csb*$^{m/m}$/*Xpa*$^{-/-}$ but not to that of *Csb*$^{m/m}$ or *Xpa*$^{-/-}$ animals (Fig. 1*F*). The strength of the *Taf10*$^{-/-}$ gene expression similarity ($r = 0.72$) to growth-defective NER mutants was comparable to that previously shown for the functionally and phenotypically interrelated *Ercc1*$^{-/-}$ and *Csb*$^{m/m}$/*Xpa*$^{-/-}$ livers ($r = 0.82$; Fig. 1*E*). Thus, the physiologic parallels between *Ercc1*$^{-/-}$ and *Taf10*$^{-/-}$ animals extend to hepatic gene expression similarities.

Venn's logic revealed that *Taf10*$^{-/-}$ livers share the great majority (77%) of *Ercc1*$^{-/-}$ gene expression changes (*SI Appendix*). *Ercc1*$^{-/-}$ livers shared a smaller percentage of significant gene expression changes (40%) with *Taf10*$^{-/-}$ livers likely reflecting additional transcriptional responses against irreparable DNA lesions not encountered by *Taf10*$^{-/-}$ livers. We then used available algorithms (*SI Appendix*) on the 1123 differentially expressed genes that showed overlapping gene expression changes between the *Ercc1*$^{-/-}$ and *Taf10*$^{-/-}$ livers. Genes related to growth, energy and detoxification metabolism (*SI Appendix*) were significantly over-represented in this gene set. Unlike the P15 *Csb*$^{m/m}$ livers, analysis on growth-defective NER mutant and *Taf10*$^{-/-}$ livers revealed, among others: a down-regulation of the somatotrophic, thyrotrophic, and lactotrophic axes, of glucose catabolism, and of cytochrome P450s; and the up-regulation of anaerobic metabolism genes and of genes involved in fatty acid synthesis and antioxidant and detoxification responses (*SI Appendix*). Thus, the *Ercc1*$^{-/-}$ and *Taf10*$^{-/-}$ liver transcriptomes are associated with biological processes that closely reflect the growth defect seen in these animals.

TFIID Is Assembled in *Ercc1*$^{-/-}$ Livers. In *Ercc1*$^{-/-}$ livers, neither the mRNA or protein levels of individual *Tafs* nor the assembly of TFIID or the mRNA levels of all basal transcription factor subunits examined were affected by ERCC1 inactivation (*SI Appendix*). We also detected similar transcript levels when using primers that amplify the N and C termini of insulin-like growth factor (*Igf1*), growth hormone receptor (*GhR*), deiodinase I (*Dio1*), and prolactin receptor (*PrlR*) RNAs (*SI Appendix*). Thus, the mRNA changes in *Ercc1*$^{-/-}$ livers are not generated by defects in TFIID integrity, aberrant processing of the pre-mRNA, or compromised mRNA stability. Similarly, in *Taf10*$^{-/-}$ livers, the XPF and ERCC1 protein levels were comparable to those seen in wild-type (wt) controls (*SI Appendix*), minimizing the possibility that the changes in *Taf10*$^{-/-}$ livers result from a constitutive defect in ERCC1-XPF.

ERCC1-XPF Is Recruited on the Promoters of Genes Associated with Postnatal Murine Growth. CS patients are characterized by postnatal growth failure (7), and genes required for postnatal growth are suppressed in murine models of CS (11, 12, 18). Based on these observations, the finding that NER factors are recruited on active promoters (15), and the physiologic and gene expression parallels between *Ercc1*$^{-/-}$ and *Taf10*$^{-/-}$ mice, we asked whether ERCC1 and its XPF partner are involved in the transcriptional activation of genes critical for somatic growth. We carried out a series of in vivo chromatin immunoprecipitation (ChIP) assays to study occupancies of the *Igf1*, *GhR*, *Dio1*, and *PrlR* promoters. These genes are essential for postnatal animal growth (17). Unlike *Ercc1*$^{-/-}$ livers, beginning on day 5, the wt livers demonstrated a robust increase in the mRNA levels of these genes (Fig. 2*A*). In wt livers, ChIP followed by qPCR showed that ERCC1 and XPF assemble with POL II and the basal transcriptional factors tested (Fig. 2*B*) on promoters but not on the −25-Kb upstream promoter regions or on the promoter of the transcriptionally inactive *GzmZ* gene (*SI Appendix*). Conversely, ChIP signals with a αFRAS1 antibody recognizing an extracellular matrix protein did not exceed background levels (Fig. 2*B*). Similar results were obtained for additional growth genes with reduced mRNA levels in *Ercc1*$^{-/-}$ livers (*SI Appendix*). Thus, ERCC1-XPF assembles together with the POL II and the basal transcription machinery on promoters of genes that are critical for postnatal murine growth.

ERCC1-XPF Is Not Required for Ongoing Hepatic Gene Transcription. Disruption of the *Ercc1* gene led to the dissociation of XPF, POL II and the basal transcription factors tested from the promoters (Fig. 2*C* and *SI Appendix*) mirroring the reduced mRNA levels seen in P15 *Ercc1*$^{-/-}$ livers (Fig. 2*A*). In P15 wt livers, we also find that XPA and XPG recruit on promoters; intriguingly, disruption of *Ercc1* did not affect the assembly of these NER factors on promoters (*SI Appendix*). In P15 wt livers, ChIP data obtained for the *Hprt* gene which expresses at high levels in fetal livers (19) and continues to be active postnatally (11, 12) showed that all of the tested factors occupied the promoter. In P15 *Ercc1*$^{-/-}$ livers,

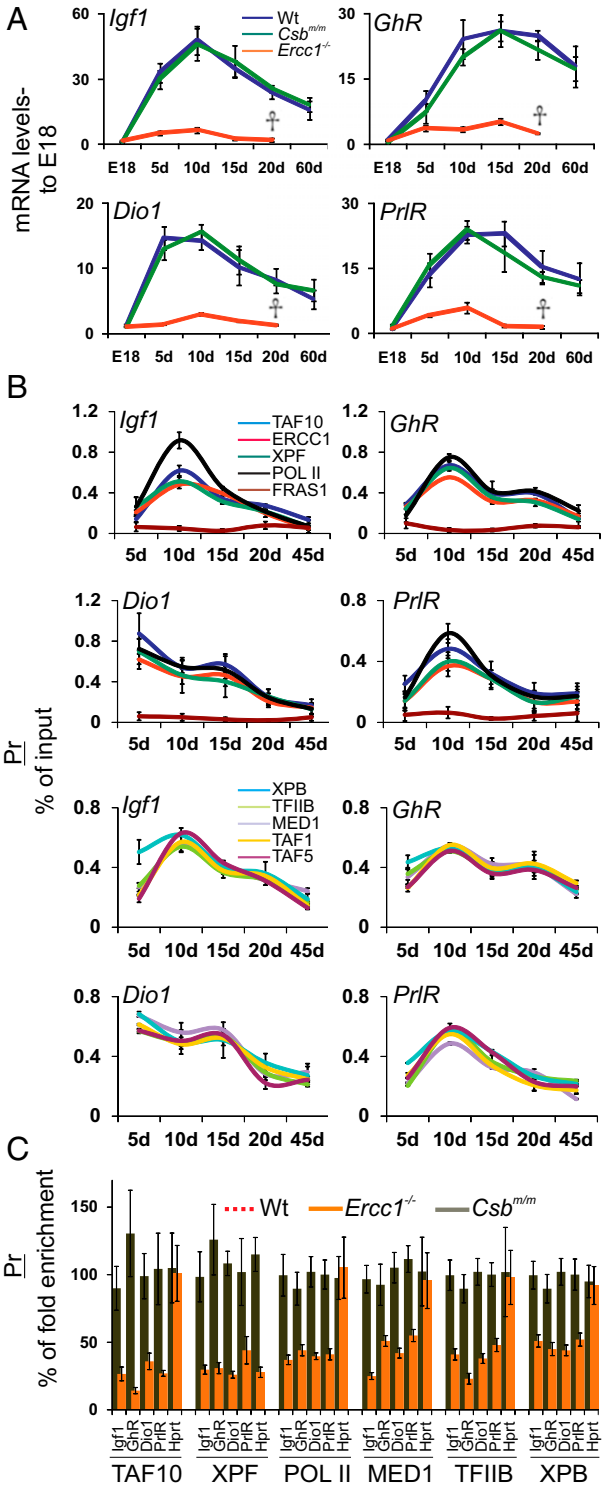

Fig. 2. ERCC1-XPF assembles on the promoters of genes associated with murine growth. (*A*) Relative *Igf1*, *GhR*, *Dio1*, and *PrlR* mRNA levels during postnatal Ercc1$^{-/-}$, *Csb*$^{m/m}$ and wt liver development ($n \geq 4$; E, embryonic; d, days). (*B*) ChIP signals of indicated promoter (Pr) regions by TAF10, ERCC1, XPF, POL II, XPB, TFIIB, MED1, TAF1, and TAF5 during wt liver development ($n \geq 4$). (*C*) ChIP assays with antibodies against the indicated factors in P15 *Ercc1*$^{-/-}$ and *Csb*$^{m/m}$ livers. The data from the qPCR reactions with primers amplifying the promoter regions of the tested genes in *Ercc1*$^{-/-}$ or *Csb*$^{m/m}$ livers ($n \geq 4$) were normalized to input and expressed as fold enrichment over those obtained from wt controls, which were set at 1 (100%; dotted horizontal line).

the *Hprt* mRNA levels and the occupancy of all factors tested on *Hprt* promoter were not significantly affected; however ChIP signals for the XPF were reduced to background levels (Fig. 2*C*). Similar results were obtained for other genes known to be actively transcribed long before birth (*SI Appendix*). Instead, ChIP signals for genes that are not expressed in P15 *Ercc1*$^{-/-}$ livers remain close to background levels (*SI Appendix*). Thus, similar to TAF10, XPF and ERCC1 are required for the optimal activation of target genes, but are dispensable for ongoing hepatic transcription.

Defects in Some NER Factors Impede the Assembly of ERCC1-XPF on Promoters. Consistent with their normal postnatal development, *Csb*$^{m/m}$ and *Xpa*$^{-/-}$ livers were proficient in the recruitment of all factors tested whereas the XPF and ERCC1 protein levels were comparable to those seen in wt controls (Fig. 2*C* and *SI Appendix*). This and the lack of a growth defect or of any detectable liver gene expression changes in P15 in *Csb*$^{m/m}$ or *Xpa*$^{-/-}$ animals (*SI Appendix*) (12) and the normative mRNA levels during postnatal *Csb*$^{m/m}$ liver development (Fig. 2*A*) suggest that CSB and XPA factors alone are not critical for the transactivation of hepatic gene targets. However, in P15 *Csb*$^{m/m}$-*Xpa*$^{-/-}$ livers, disruption of both *Csb* and *Xpa* led to the dissociation of all factors tested from promoters (*SI Appendix*), closely mirroring the reduced *Igf1*, *GhR*, *Dio1*, and *PrlR* mRNA levels and the severe growth defect seen in these animals (12). As TFIIH is involved in both NER and transcription (13), we also asked whether the ChIP signals on promoters for ERCC1-XPF reflect the physical proximity of this complex to TFIIH during NER. However, a genome-wide expression analysis in P15 *Xpd*^{TTD} livers, which carry a R722W mutation in the mouse *Xpd* gene (13), revealed no gene expression changes associated with growth or energy metabolism (Fig. 3 *A* and *B* and *SI Appendix*). In agreement with this result, P15 *Xpd*^{TTD} animals are not growth-defective (13).

To test whether the TFIID complex interacts with ERCC1-XPF, we isolated ERCC1-containing protein complexes by in vivo biotinylation tagging and direct binding to streptavidin beads. Human embryonic kidney (HEK) 293 cells were cotransfected with an N-terminal avidin-tag fused version of murine ERCC1 (bERCC1) and a biotin ligase (BirA) expression vector. BirA specifically recognizes and biotinylates the short tag, thus creating a very high affinity "handle" for isolating tagged ERCC1 by binding to streptavidin. Nuclear extracts were incubated with streptavidin-coated beads and subjected to Western blot analysis with antibodies raised against ERCC1, TBP, several TAFs (Fig. 3 *C* and *D*), and known protein partners XPF and XPA (*SI Appendix*). Our analysis revealed that bERCC1 interacts with TAF6, TAF7, TAF10, TAF12 and TBP (Fig. 3*D*) but less so with TAF4 or TAF5 (*SI Appendix*). ChIP with αTAF6, αTAF10 and αTAF12 antibodies and Western blot experiments with αERCC1 in wt livers further confirmed these findings (*SI Appendix*). Interestingly, ChIP signals for ERCC1 and XPF on promoters in *Taf10*$^{-/-}$ livers were reduced to background levels, suggesting that interaction with distinct TAFs targets ERCC1-XPF to gene promoters (*SI Appendix*).

ERCC1-XPF Facilitates Transcription Initiation in Vitro. To test whether ERCC1-XPF is directly involved in transcription activation, naive primary wt embryonic fibroblasts (MEFs) were exposed for 13 d to an adipogenic stimulus. This led to the robust increase in the mRNA levels of *adipoQ* and *adipsin* genes encoding two protein hormones secreted by differentiated adipocytes (20) (Fig. 3*E*) and to the de novo lipid accumulation marking the generation of differentiated, functional adipocytes (Fig. 3*F*). In contrast, exposure of *Ercc1*$^{-/-}$ MEFs to adipogenic media had no effect in the *adipoQ* and *adipsin* mRNA levels (Fig. 3*E*) and resulted in the nearly complete absence of productive lipid accumulation (Fig. 3*F Lower*). Forty-eight-hour treatment of wt primary MEFs with adipogenic media led to the assembly of XPF and POL II on promoters of these genes but

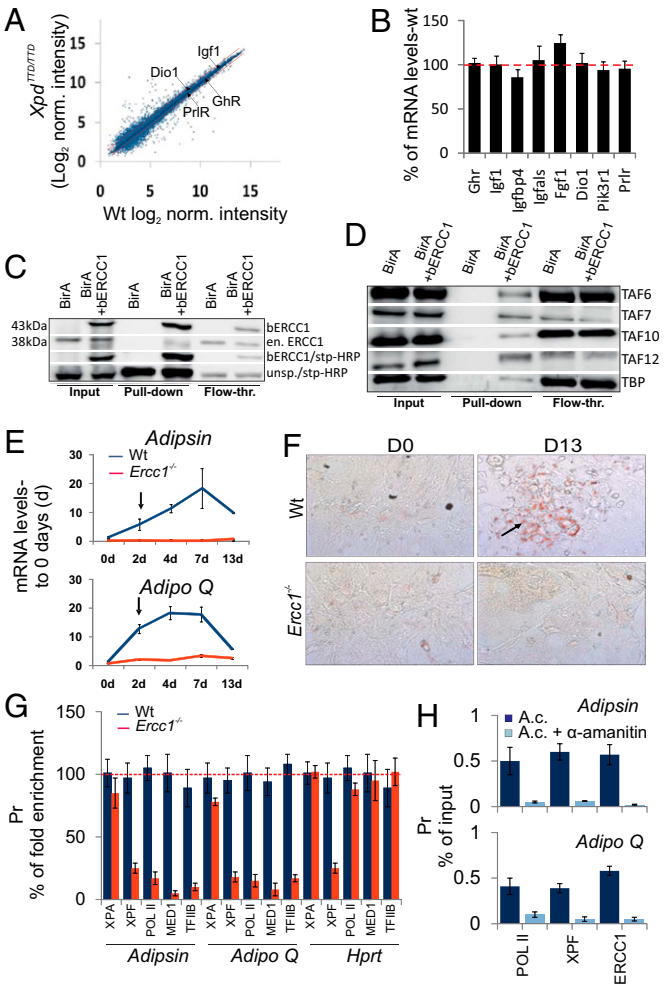

Fig. 3. Recruitment of ERCC1-XPF on promoters during adipogenesis. (*A*) Scatter plot of normalized (norm.) microarray hybridization signals obtained from P15 Xpd^{TTD} liver RNA samples versus wt controls (*SI Appendix*). (*B*) qPCR evaluation of mRNA levels of genes representing the GH/IGF1 axis and mitogenic signals in P15 Xpd^{TTD} livers. For each gene, expression levels in the Xpd^{TTD} livers are plotted relative to those of age-matched controls (red dotted line). Error bars indicate SEM between replicates ($n \geq 4$). (*C*) Nuclear extracts from HEK 293 cells expressing both bERCC1 and BirA biotin ligase were tested by Western blot. The blot was probed with αERCC1 antibody revealing bands corresponding to the biotin-tagged (b)ERCC1 (top band) and the endogenous ERCC1 (en. ERCC1) as well as with streptavidin-HRP (stp-HRP) probe, which confirms biotinylation of ERCC1 (bERCC1). Endogenously unspecific (unsp.) biotinylated proteins detected by streptavidin-HRP probe were used as loading control (lower lane). (*D*) bERCC1 pull downs analyzed by Western blotting for TBP and the indicated TAFs. The input and flow-through are 1/15 and 1/20 of the extract used, respectively. (*E*) *Adipsin* and *AdipoQ* mRNA levels in wt and $Ercc1^{-/-}$ MEFs after exposure to adipogenic stimulus compared with day 0 (d: days; arrow indicates the 48-h time point for ChIP assays shown in Fig. 2 *E*–*G*). (*F*) Oil Red O staining (arrow) of wt and $Ercc1^{-/-}$ MEFs subjected to adipogenic stimulation (D: days). (*G*) ChIP signals for promoters (as shown) with antibodies against the indicated factors in $Ercc1^{-/-}$ and wt MEFs exposed to 48 h of adipogenic stimulus. The data are presented as in Fig. 2*C*. Scale bars show mean values and SDs from at least four independent experiments. (*H*) POLII, XPF, and ERCC1 ChIP signals on promoters (as shown) in wt MEFs exposed for 12 h to adipogenic mixture (Ac) in the absence (dark blue) or presence (light blue) of α-amanitin (10 μg/mL).

not on the −25-Kb upstream promoter regions (*SI Appendix*) matching the onset of increase in mRNA levels (Fig. 3*E*). In $Ercc1^{-/-}$ MEFs, ChIP signals for XPF, POL II, MED1, and TFIIB on promoters were markedly reduced compared with wt MEFs (Fig. 3*G*). Under these conditions, we also found that XPA assembles on *adipoQ* and *adipsin* promoters; although XPA ChIP signals for the *adipoQ* and *adipsin* promoters in $Ercc1^{-/-}$ MEFs were slightly reduced compared with wt MEFs, they were not abolished. Consistent with the high expression of the *Hprt* gene in $Ercc1^{-/-}$ MEFs (21), POL II, MED1, and TFIIB occupied this promoter, whereas ChIP signals for XPF were substantially reduced compared with wt MEFs (Fig. 3*G*). To demonstrate that the recruitment of ERCC1-XPF on promoters reflects a real association with the transcription machinery, wt MEFs were simultaneously exposed for 12 h to the transcription inhibitor α-amanitin and the adipogenic stimulus. This led to the inhibition of *adipsin* and *adipoQ* mRNA synthesis (*SI Appendix*). Neither POL II nor XPF or ERCC1 were detected on the *adipoQ* and the *adipsin* promoters (Fig. 3*H*). We also monitored the responsiveness of *adipoQ* and *Igf1* promoters to ERCC1 and XPF by transiently cotransfecting pCMV-bErcc1 (Fig. 3*C*) or pCMV-bXpf (*SI Appendix*) together with the *adipoQ* or *Igf1* luciferase promoter plasmids in NIH 3T3 cells. In line, the binding of ERCC1 and XPF factors on *adipoQ* and *Igf1* promoter plasmids significantly increased the promoter-driven luciferase activities (*SI Appendix*) further supporting the role of ERCC1-XPF in transcription activation.

Assembly of ERCC1-XPF on Promoters Is Accompanied by DNA Demethylation and Histone Marks Associated with Active Transcription. Gadd45a interacts with and requires XPG to facilitate promoter demethylation during transcription (22). In this work, we find that, Gadd45a assembles on promoters but not on the −25-Kb upstream promoter regions of growth genes or on the promoter of the transcriptionally inactive *GzmZ* gene (*SI Appendix*) during liver development. Unlike $Csb^{m/m}$ livers, disruption of *Ercc1* led to the dissociation of Gadd45a from promoters (*SI Appendix*). Thus, Gadd45a assembles on promoters during hepatic development; a defect in *Ercc1*, but not in *Csb*, substantially affects the recruitment of Gadd45a on promoters.

Using a methylation-sensitive ChIP approach (ChIP-chop) (23), we next sought to evaluate whether DNA methylation interferes with the assembly of ERCC1-XPF and Gadd45a on promoters. Before qPCR, the input, ERCC1-, XPF- and Gadd45a-enriched DNA samples derived from wt livers were digested with the methylation-sensitive *HpaII* and methylation-insensitive *MspI* restriction enzymes. Beginning day 5, we noticed a high content of *HpaII*-resistant input DNA (i.e., methylation) on promoters that gradually decreased reaching a minimum signal at ∼P15 (i.e., demethylation) (Fig. 4*A*). As shown by the "ChIP-chop" comparative analysis of input versus ERCC1- or XPF-bound DNA fragments, ERCC1 did not bind DNA in a methylation-sensitive manner; XPF showed a small preference toward binding nonmethylated DNA (*SI Appendix*). Instead, Gadd45a was preferentially assembled on nonmethylated DNA (*SI Appendix*). Unlike the P15 $Csb^{m/m}$ livers, disruption of the *Ercc1* gene in $Ercc1^{-/-}$ livers led to the aberrant DNA methylation on promoters compared with age-matched wt livers (Fig. 4*B* and *SI Appendix*). Thus, the presence of ERCC1-XPF on promoters is accompanied by promoter DNA demethylation with Gadd45a protein binding preferentially nonmethylated DNA. A similar analysis on the *Hprt* promoter in all of the animal models tested revealed no difference in the content of *HpaII*-resistant DNA of input and ChIP samples (*SI Appendix*).

Examination of the chromatin status in P15 $Ercc1^{-/-}$ livers revealed a loss of activating acetylated histone H3Ac and H3K4 trimethylation and a concomitant increase of repressive histone H3K9 dimethylation and H3K27 trimethylation marks with promoter-specific requirements (Fig. 5*A*). At the *Dio1* and *PrlR* promoters, a decrease in the acetylation of histone 3 and H3K4 trimethylation was accompanied by a significant increase in H3K27 trimethylation and H3K9 dimethylation; at the *Igf1* and *GhR* promoters, a decrease of H3Ac and H3K4me3 ChIP signals coincided with an increase of H3K27me3 but not H3K9me2 ChIP signals (Fig. 5*A*). Thus, ERCC1-XPF assembly on promoters is accompanied by active DNA demethylation and histone post-translational modifications associated with active transcription.

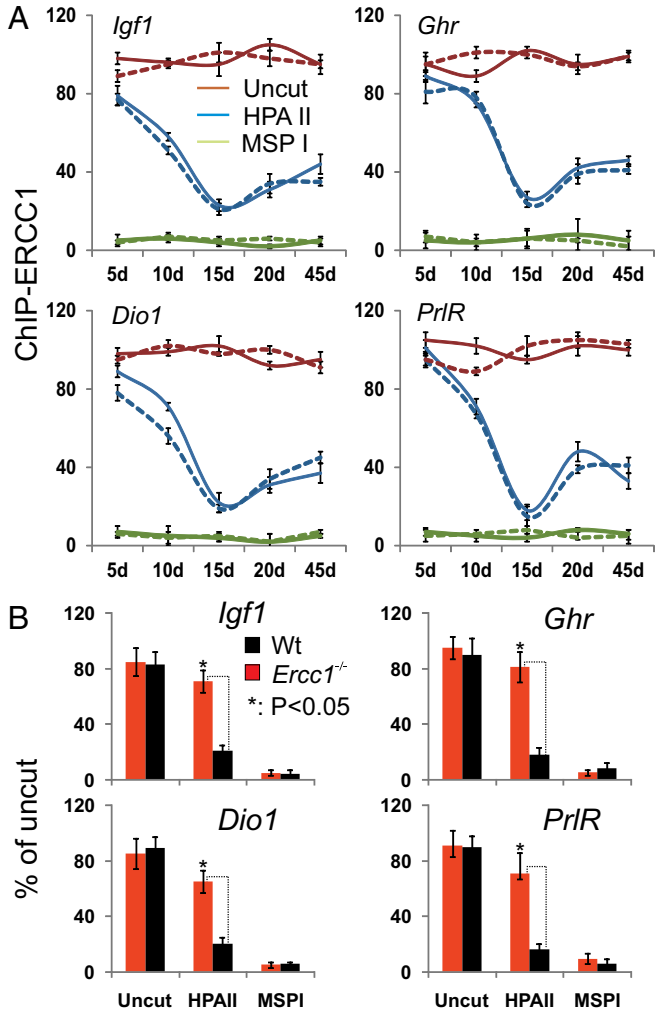

Fig. 4. Assembly of ERCC1-XPF on promoters is accompanied by DNA demethylation. (*A*) Methylation-sensitive ChIP-qPCR signals of input (solid line) and ERCC1-enriched DNA samples (dotted line) digested with *HpaII*, *MspI*, or left undigested during wt liver development. For each promoter, the percentage of *HpaII* or *MspI* digestion resistance is represented as a percentage of mock digested DNA (*y* axis). (*B*) Methylation-sensitive qPCR signals of DNA samples in P15 $Ercc1^{-/-}$ livers compared to controls.

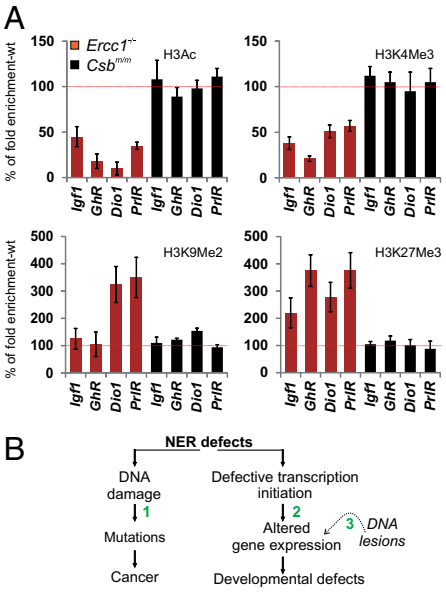

Fig. 5. Histone posttranslational modifications in $Ercc1^{-/-}$ and $Csb^{m/m}$ livers. (*A*) ChIP signals for activating (H3Ac, H3K4Me3) and repressive (H3K9Me2, H3K27Me3) histone modifications at the indicated promoter regions in P15 $Ercc1^{-/-}$ and $Csb^{m/m}$ livers ($n \geq 4$). The data are presented as shown in Fig. 2*C*. (*B*) A model integrating the dual function of NER in DNA repair and transcription initiation: ERCC1-XPF together with other NER factors functions beyond NER in the transcriptional activation of developmental stage- and tissue-specific gene expression programs. The presence of irreparable DNA lesions (due to, for example, defective NER) may further aggravate the pathological outcome of NER abnormalities.

Discussion

Why some, but not all, defects in NER lead to developmental abnormalities and how such pathological outcomes manifest in some, but not all, organs remains an intriguing question that argues for distinct NER factors having tissue-specific functions beyond NER (15). Here, we provide in vivo evidence that the severe growth retardation seen in $Ercc1^{-/-}$ animals originates from defective transcription initiation of developmental gene expression programs.

Defect in Transcription Initiation Recapitulates the Growth Defect in $Ercc1^{-/-}$ Animals. Both the NER progeroid $Ercc1^{-/-}$ and TFIID-defective $Taf10^{-/-}$ mice are growth defective, show noticeable liver apoptosis, have a marked propensity to store rather than burn glycogen and fat, die before weaning, and share unusually similar hepatic gene expression profiles. Strikingly, the latter reflects more the severity of growth retardation rather than the DNA-repair defect in NER. The extensive parallels between these otherwise distinct mouse strains occur in the absence of a TFIID deficiency in $Ercc1^{-/-}$ livers or of an ERCC1-XPF defect in $Taf10^{-/-}$ livers. Instead, we find that ERCC1-XPF assembles with the basal transcription machinery on promoters during liver development. Failure of ERCC1-XPF to do so results in defective transcription initiation of genes critical for postnatal growth.

Given the known role of CSB and XPD in transcription (24, 25) and the fact that XPA is upstream of ERCC1 in the canonical NER pathway, it is surprising that none of these proteins alone are required for the initial activation of hepatic genes; recruitment of ERCC1-XPF on promoters requires the concurrent availability of CSB and XPA factors (as shown in $Csb^{m/m}$-$Xpa^{-/-}$ livers). However, TFIIH and likely also CSB may only be partially defective in Xpd^{TTD} and $Csb^{m/m}$ livers, respectively. We also find that ERCC1-XPF is dispensable for ongoing transcription; unlike POL II or any of the factors tested, ChIP signals for genes whose high expression levels remain unaltered in $Ercc1^{-/-}$ livers revealed a complete dissociation of ERCC1-XPF from promoters (Fig. 2*C* and *SI Appendix*). Our finding that distinct TAFs and TBP physically interact with ERCC1 may explain how ERCC1-XPF is specifically recruited to the promoters of active genes. Interestingly, the contribution of ERCC1-XPF to the de novo initiation of hepatic transcription extends to genes promoting adipogenesis; assembly of ERCC1-XPF on promoters was also sensitive to the transcription inhibitor α-amanitin. Finally, ERCC1 and XPF significantly increase the activity of *adipoQ* and *Igf1* promoter-driven luciferase activities in transiently transfected NIH 3T3 cells (*SI Appendix*).

ERCC1-XPF Complex Functions in Transcription Initiation Beyond NER. In view of the NER defect, one could envision that at least some of the $Ercc1^{-/-}$ liver gene expression changes originate from the presence of irreparable DNA lesions. Indeed, DNA lesions would further aggravate the transcriptional defect in $Ercc1^{-/-}$ animals or, in certain instances, increased DNA damage levels could compromise the availability of ERCC1-XPF aimed for transcription initiation during hepatic development (Fig. 5*B*). Moreover, the NER defect alone could account for the numerous progressive hepatic symptoms associated with aging in $Ercc1^{-/\Delta}$ mice that are healthy into adulthood and live substantially longer than the

GENETICS

growth-defective, short-lived *Ercc1*$^{-/-}$ and *Taf10*$^{-/-}$ animals (26). Mutations in ERCC1, XPF, and XPG represent the only single-gene defects known in NER that are associated with growth attenuation and death before weaning in mice (27). However, several double NER mutant mice are also associated with cachectic dwarfism and, for the animal models tested so far, their P15 hepatic gene expression changes are exceptionally similar to those seen in *Taf10*$^{-/-}$ or *Ercc1*$^{-/-}$ livers (11, 12, 18). This surprising requirement of certain, but not all, NER factors in the transcription initiation of hepatic genes during development contrasts with the UV sensitivity seen in XP, CS, and TTD patients; whereas the latter depends on the DNA repair defect, the former likely reflects a transcriptional defect during development.

Recruitment of ERCC1-XPF on Promoters Is Accompanied by DNA Demethylation and Histone Posttranslational Modifications. Despite the controversial involvement of Gadd45a in active promoter DNA demethylation (22, 28), we found that Gadd45a assembles together with ERCC1-XPF on promoters. Recruitment of ERCC1-XPF on promoters was followed by DNA demethylation on promoter-proximal DNA closely mirroring the peak of mRNA levels during development. Instead, a defect in *Ercc1*, but not in *Csb*, led to aberrant promoter DNA methylation. TAF12 was recently shown to recruit Gadd45a and the NER complex to the promoter of rRNA genes leading to active DNA demethylation (29). These findings point to a similar role for TAFs and ERCC1-XPF during POL II-mediated transcription. Consistently, the aberrant promoter-proximal DNA methylation in P15 *Ercc1*$^{-/-}$ livers was associated with a decrease of activating H3Ac and H3K4me3 histone marks and a concomitant enrichment in trimethylation of H3K27 more than H3K9 dimethylation. With the exception of a mild increase in H3K9 dimethylation on *Dio1* promoter, the P15 *Csb*$^{m/m}$ livers showed none of the *Ercc1*$^{-/-}$-associated histone marks on promoters.

Conclusions

In summary, we find that, upon gene activation, ERCC1-XPF recruits together with the RNA POL II and the basal transcription machinery at the promoters of hepatic genes. Assembly of ERCC1-XPF on promoters is followed by histone marks and promoter proximal DNA demethylation associated with active transcription. Whereas the role of XPG, TFIIH and CSB in POL II-mediated transcription has been well documented (30), it has been difficult to envisage a role for ERCC1-XPF in transcription initiation in vivo. Our data are in line with previous findings on XPG (22), supporting a similar role for ERCC1-XPF in facilitating repair-mediated active DNA demethylation on promoters. Interaction of ERCC1-XPF complex with specific TAFs during gene activation also suggests that this complex acts as a coactivator during the transcription process. This is in line with the fact that TBP/TAF complexes often recruit various classes of coactivators to execute specific transcriptional programs (1, 31) as well as the recently proposed function of the XPC/RAD23B/CETN2 NER complex in the maintenance and re-establishment of stem cell pluripotency (14). Thus, although ERCC1/XPF may not be essential for initiating basal transcription itself, it is required for the fine-tuning of optimal transactivation of target genes. The period at which NER factors optimize transcription during postnatal development may well explain the heterogeneous and tissue-specific pathology of NER syndromes. It is, therefore, attractive to speculate that the so called "segmental" NER progeroid features may also reflect the "segmental" transcriptional requirements for certain NER factors during mammalian development.

Methods

Information on the animal models used is shown in *SI Appendix*. Cell culturing, the Periodic Acid Schiff, Oil Red O, and TdT-mediated dUTP Nick-End Labeling were performed as previously described (12, 21). Microarrays, qPCRs, and data analysis were performed as previously described (21). Detailed information on in vivo biotinylation tagging approach and the reporter gene assays is shown in *SI Appendix*. Westerns blots, ChIP, coimmunoprecipitation assays, and the methylation-sensitive ChIP assay were performed as previously described (16, 23).

ACKNOWLEDGMENTS. We thank Prof. J. H. J. Hoeijmakers and Dr. B. Schumacher for critical discussions on the manuscript, Dr. G. T. J. van der Horst for *Ercc1*$^{-/-}$ and *Csb*$^{m/m}$ animals, Dr L. Tora for *Taf10*$^{lox/lox}$ mice, Dr. G. Chalepakis for αFRAS1 antibody, and Dr. J. Strouboulis for the in vivo biotinylation tagging constructs. This work was supported by Capacities-FP7-REGPOT-2008-1 "ProFI", the National Strategic Reference Framework 2007-2013 "Herakleitos II (KA3396)", and "Cooperation" No. EDGE 901-13/11/2009 programs.

1. Lemon B, Tjian R (2000) Orchestrated response: A symphony of transcription factors for gene control. *Genes Dev* 14:2551–2569.
2. Ohler U, Wassarman DA (2010) Promoting developmental transcription. *Development* 137:15–26.
3. Hoeijmakers JH (2001) Genome maintenance mechanisms for preventing cancer. *Nature* 411:366–374.
4. Hanawalt PC (2002) Subpathways of nucleotide excision repair and their regulation. *Oncogene* 21:8949–8956.
5. Lainé JP, Egly JM (2006) When transcription and repair meet: A complex system. *Trends Genet* 22:430–436.
6. Cleaver JE (2005) Cancer in xeroderma pigmentosum and related disorders of DNA repair. *Nat Rev Cancer* 5:564–573.
7. Bootsma D, Kraemer KH, Cleaver JE, Hoeijmakers JHJ (1998) Nucleotide excision repair syndromes: Xeroderma pigmentosum, Cockayne syndrome and trichothiodystrophy. *The genetic basis of human cancer*, eds Vogelstein B, Kinzler KW (McGraw-Hill, New York), pp 245–274.
8. Hoeijmakers JH (2009) DNA damage, aging, and cancer. *N Engl J Med* 361:1475–1485.
9. Schumacher B, Garinis GA, Hoeijmakers JH (2008) Age to survive: DNA damage and aging. *Trends Genet* 24:77–85.
10. Garinis GA, van der Horst GT, Vijg J, Hoeijmakers JH (2008) DNA damage and ageing: New-age ideas for an age-old problem. *Nat Cell Biol* 10:1241–1247.
11. Niedernhofer LJ, et al. (2006) A new progeroid syndrome reveals that genotoxic stress suppresses the somatotroph axis. *Nature* 444:1038–1043.
12. van der Pluijm I, et al. (2007) Impaired genome maintenance suppresses the growth hormone—insulin-like growth factor 1 axis in mice with Cockayne syndrome. *PLoS Biol* 5:e2.
13. de Boer J, et al. (2002) Premature aging in mice deficient in DNA repair and transcription. *Science* 296:1276–1279.
14. Fong YW, et al. (2011) A DNA repair complex functions as an Oct4/Sox2 coactivator in embryonic stem cells. *Cell* 147:120–131.
15. Le May N, et al. (2010) NER factors are recruited to active promoters and facilitate chromatin modification for transcription in the absence of exogenous genotoxic attack. *Mol Cell* 38:54–66.
16. Tatarakis A, et al. (2008) Dominant and redundant functions of TFIID involved in the regulation of hepatic genes. *Mol Cell* 31:531–543.
17. Schumacher B, et al. (2008) Delayed and accelerated aging share common longevity assurance mechanisms. *PLoS Genet* 4:e1000161.
18. van de Ven M, et al. (2006) Adaptive stress response in segmental progeria resembles long-lived dwarfism and calorie restriction in mice. *PLoS Genet* 2:e192.
19. Duncan SA (2000) Transcriptional regulation of liver development. *Dev Dyn* 219: 131–142.
20. Gupta RK, et al. (2010) Transcriptional control of preadipocyte determination by Zfp423. *Nature* 464:619–623.
21. Garinis GA, et al. (2009) Persistent transcription-blocking DNA lesions trigger somatic growth attenuation associated with longevity. *Nat Cell Biol* 11:604–615.
22. Barreto G, et al. (2007) Gadd45a promotes epigenetic gene activation by repair-mediated DNA demethylation. *Nature* 445:671–675.
23. van de Nobelen S, et al. (2010) CTCF regulates the local epigenetic state of ribosomal DNA repeats. *Epigenetics Chromatin* 3:19.
24. Balajee AS, May A, Dianov GL, Friedberg EC, Bohr VA (1997) Reduced RNA polymerase II transcription in intact and permeabilized Cockayne syndrome group B cells. *Proc Natl Acad Sci USA* 94:4306–4311.
25. Iyer N, Reagan MS, Wu KJ, Canagarajah B, Friedberg EC (1996) Interactions involving the human RNA polymerase II transcription/nucleotide excision repair complex TFIIH, the nucleotide excision repair protein XPG, and Cockayne syndrome group B (CSB) protein. *Biochemistry* 35:2157–2167.
26. Gregg SQ, et al. (2011) A mouse model of accelerated liver aging due to a defect in DNA repair. *Hepatology*, 10.1002/hep.24713.
27. Niedernhofer LJ (2008) Nucleotide excision repair deficient mouse models and neurological disease. *DNA Repair (Amst)* 7:1180–1189.
28. Jin SG, Guo C, Pfeifer GP (2008) GADD45A does not promote DNA demethylation. *PLoS Genet* 4:e1000013.
29. Schmitz KM, et al. (2009) TAF12 recruits Gadd45a and the nucleotide excision repair complex to the promoter of rRNA genes leading to active DNA demethylation. *Mol Cell* 33:344–353.
30. Le May N, Egly JM, Coin F (2010) True lies: The double life of the nucleotide excision repair factors in transcription and DNA repair. *J Nucleic Acids* 2010:2010.
31. Näär AM, et al. (1998) Chromatin, TAFs, and a novel multiprotein coactivator are required for synergistic activation by Sp1 and SREBP-1a in vitro. *Genes Dev* 12: 3020–3031.